

Superconducting Nanocomposites: Enhancement of Bulk Pinning and Improvement of Intergrain Coupling

Ruslan Prozorov, Tanya Prozorov, and Alexey Snezhko

Abstract—Heterogeneous sonochemical method was applied for synthesis of novel superconducting nanocomposites consisting of magnetic (and/or nonmagnetic) nanoparticles embedded into the bulk of ceramic superconductors. In addition to in-situ production of the efficient pinning centers, this synthesis method considerably improves the intergrain coupling. Significant enhancement of the magnetic irreversibility is reported for Fe_2O_3 nanoparticles embedded into the bulk of MgB_2 superconductor. Nonmagnetic Mo_2O_5 nanoparticles also increase pinning strength, but less than magnetic Fe_2O_3 . Detailed magnetization and electron microscopy characterization is presented. Theory of bulk magnetic pinning due to ferromagnetic nanoparticles of finite size embedded into the superconducting matrix is developed.

Index Terms—Ferromagnetic nanoparticle, intergrain current, magnesium diboride, vortex pinning.

I. INTRODUCTION

CRITICAL current density is the key parameter determining useful applications of superconductors [1]. Although theoretically it is much easier to deal with perfect crystals, they have little practical use. Thin films are capable of carrying large current densities, but the total current remains very small. Bulk superconductors are very attractive from this point of view. Indeed, it is desirable to use superconductors with elevated transition temperatures. Unfortunately, high- T_c superconductors are granular ceramics and modification of their morphological and chemical properties is much more difficult compared to conventional metallic alloys.

Among variety of methods developed to enhance pinning in superconductors, only few can be used for bulk ceramic materials. Conventional mechanical cold-working is not applicable due to brittleness; irradiation with heavy ions is inefficient due to small ion penetration depth; thermal cycling does not generally lead to the same results as in alloys (e.g. Nb-Ti). Most efficient ways to increase pinning in ceramic superconductors are

chemical and thermal modifications of grain morphology, or deliberate introduction of nonsuperconducting pinning centers. A serious problem and uncertainty arises due to interplay of bulk and grain-boundary pinning and current percolation. Therefore, it is desirable to develop experimental treatments that *simultaneously* enhance intergrain coupling and increase bulk pinning.

This paper describes a novel way to achieve these effects by using heterogeneous sonochemical synthesis. In materials, such as Bi-Sr-Ca-Cu-O, critical current density is mostly determined by the intergrain coupling [2], whereas oxygen content sensitivity of Y-Ba-Cu-O imposes serious constraints on the methods of pinning enhancements. The method is demonstrated on MgB_2 superconductor that has two advantages compared to its higher- T_c confreres. First, the irreversible properties of MgB_2 are mostly determined by the bulk in-grain pinning forces and, second, it is an s-wave superconductor [3]. The latter is important for the suggested use of ferromagnetic nanoparticles as pinning centers, because s-wave superconductors are much less sensitive to magnetism compared to *d*-wave cuprates.

Traditional nonmagnetic and nonsuperconducting pinning centers utilize recovery of the condensation energy loss. However, as shown below, if such defects are made ferromagnetic, the net pinning becomes even stronger. The enhancement of pinning by ferromagnetic nanoparticles was demonstrated in conventional superconductors in 60s [4]–[6] and more recent works studied this effect in thin films and on surfaces of low- T_c superconductors [7]–[9]. The present work explores distinctly different approach: *bulk* pinning due to finite-size *ferromagnetic nanoparticles* embedded into *ceramic superconductors*. To the best of our knowledge, this was not studied before—neither experimentally, nor theoretically [10]–[12].

II. EXPERIMENTAL

A. Sonochemical Synthesis of Nanocomposites

Acoustic cavitation induced by intense ultrasound produces violent turbulence and shock waves. The implosive collapse of bubbles during cavitation results in extremely high local temperatures (~ 5000 K), high pressures (~ 800 atm), but for very short times (< 100 ns) which leads to high cooling rates, about $\sim 10^{10}$ K/s [13]–[15]. Shockwaves stimulate high-velocity collisions between suspended particles with the effective temperatures sufficient to partially melt collided particles, which causes localized inter-particle welding and “neck” formation [13], [14]. The estimated speed of colliding

Manuscript received October 4, 2004. This work was supported in part by the donors of the American Chemical Society Petroleum Research Fund and USC Research and Productive Scholarship Award.

R. Prozorov is with the Department of Physics and Astronomy, University of South Carolina, Columbia, SC 29208 USA (e-mail: prozorov@sc.edu).

T. Prozorov is with the Department of Chemical Engineering, University of South Carolina, Columbia, SC 29208 USA (e-mail: prozorot@enr.sc.edu).

A. Snezhko is with the Department of Physics and Astronomy, University of South Carolina, Columbia, SC 29208 USA and is now with the Materials Science Division, Argonne National Laboratory, Argonne, IL 60439 USA (e-mail: snezhko@anl.gov).

Digital Object Identifier 10.1109/TASC.2005.848851

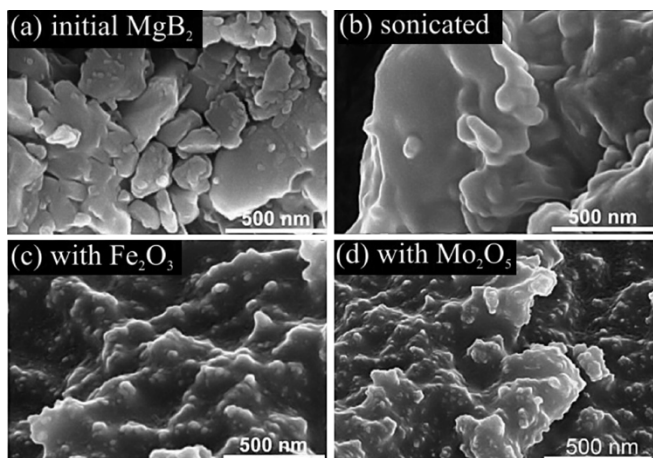


Fig. 1. Scanning electron microscope images of (a) initial MgB_2 powder; (b) sonicated MgB_2 ; (c) MgB_2 sonicated with $\text{Fe}(\text{CO})_5$; (d) MgB_2 sonicated with $\text{Mo}(\text{CO})_6$.

particles approaches half of the speed of sound. In our experiments, MgB_2 polycrystalline powder was ultrasonically irradiated for 60 min at -5°C in 15 ml of decalin (0.1–2%wt slurry loading, at 20 kHz and $\sim 50 \text{ W}/\text{cm}^2$) under ambient atmosphere using direct-immersion ultrasonic horn (*Sonics VCX-750*). Similar sets of slurries were sonicated with 1.8 mmol of $\text{Fe}(\text{CO})_5$ to produce superconductor—ferromagnetic nanoparticle $\text{MgB}_2 - \text{Fe}_2\text{O}_3$ nanocomposites. Similarly, MgB_2 slurries were sonicated with 1.8 mmol of $\text{Mo}(\text{CO})_6$ to produce nonmagnetic Mo_2O_5 pinning centers.

Fig. 1 shows scanning electron microscope images of the (a) initial MgB_2 powder, (b) sonicated MgB_2 , (c) MgB_2 sonicated with $\text{Fe}(\text{CO})_5$ that produced embedded 5–50 nm Fe_2O_3 nanoparticles, (d) MgB_2 sonicated with $\text{Mo}(\text{CO})_6$ resulted in embedded nonmagnetic Mo_2O_5 nanoparticles. The dramatic change of morphology due to sonication is obvious. Material becomes more compact with fused together grains. Small “knobs” visible in Fig. 1(c) and (d) are Fe_2O_3 and Mo_2O_5 particles and agglomerates of such particles. To support this statement, local energy dispersive x-ray spectroscopy (EDX) was performed. Fig. 2(a) shows EDX spectra for initial sample and sonicated sample. With the except for small amount of Ti, coming from the abrasion of ultrasonic horn, and increased percentage of oxygen due to sonication under ambient atmosphere, the two spectra are identical. Fig. 2(b) shows spectra collected from nanocomposite with Fe_2O_3 nanoparticles. An on-spot spectrum is compared to the off-spot spectrum (locations are shown in the inset). Clearly, the spot (or “knob”) contains significant amount of Fe, whereas off-spot area is analogous to that Fig. 2(a) showing sonicated MgB_2 . Similar situation is observed in Fig. 2(c) which shows MgB_2 with Mo_2O_5 nanocomposite. These measurements firmly support our conclusion that described technique a) produces highly compact material with b) nanosized pinning centers embedded into the bulk of ceramic superconductor.

B. Irreversible Magnetic Properties

To verify that structural modifications result in desirable changes of superconducting properties, magnetic response was

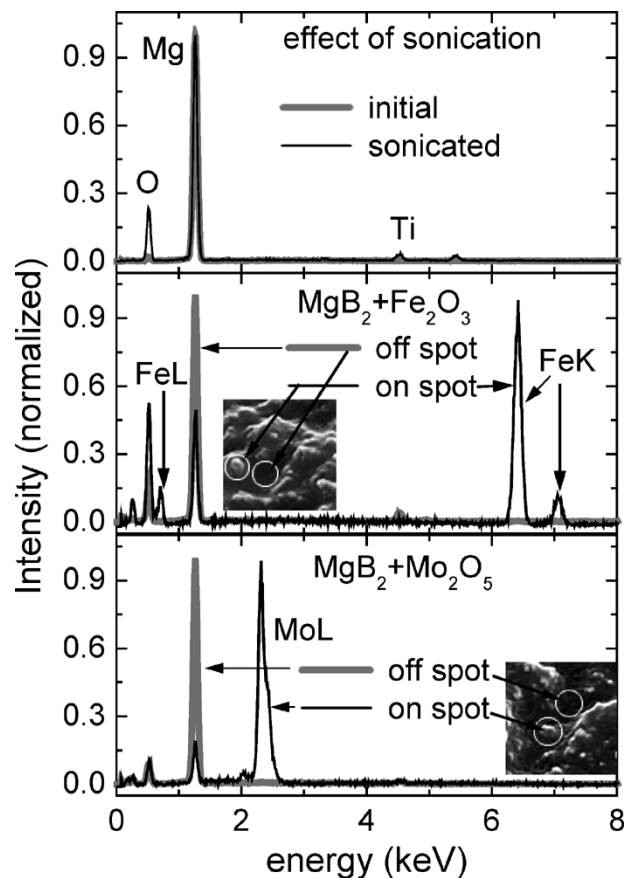


Fig. 2. Local energy dispersive x-ray (EDX) spectra obtained in (a) initial and sonicated samples; (b) $\text{MgB}_2 + \text{Fe}_2\text{O}_3$ nanocomposite—spectra measured on a spot (shown in the inset) compared to the off-spot spectra; (c) $\text{MgB}_2 + \text{Mo}_2\text{O}_5$ measurements similar to (b) above.

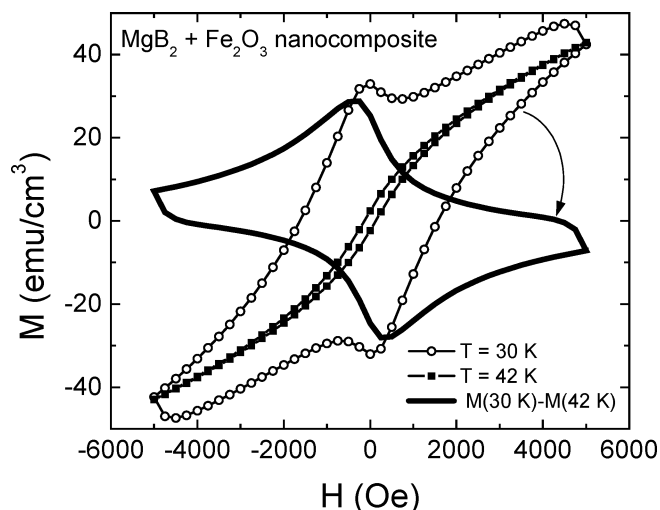


Fig. 3. Magnetization as a function of applied field in $\text{MgB}_2 + \text{Fe}_2\text{O}_3$ nanocomposite measured at 30 K (open circles) shown together with $M(H)$ curve measured above T_c , at 42 K (solid squares). Solid line is the subtracted magnetization loop.

measured by using *Quantum Design* MPMS magnetometer. All samples were cold-pressed from powders at 2.5 GPa for 12 hours to form 1.5 mm thick pellets of 6.4 mm in diameter. For measurements $1.5 \times 3 \times 6 \text{ mm}^3$ slabs were cut from the pellets. Fig. 3 shows magnetization loops measured

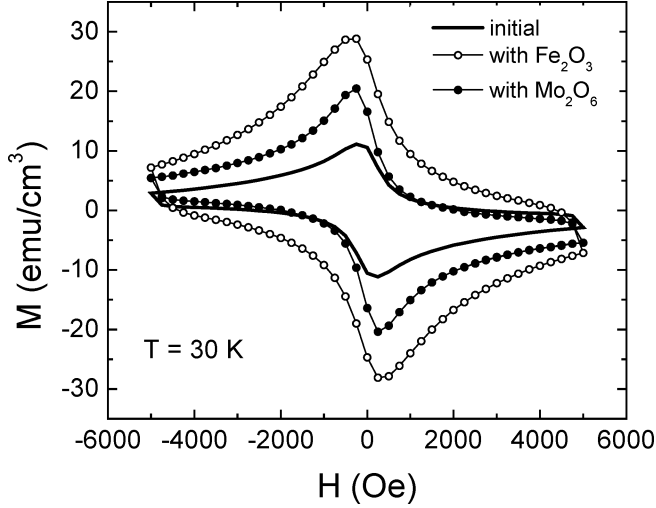


Fig. 4. Comparison of the magnetization loops at 30 K for initial material (solid curve), $\text{MgB}_2 + \text{Mo}_2\text{O}_5$ nanocomposite (solid symbols) and $\text{MgB}_2 + \text{Fe}_2\text{O}_3$ nanocomposite (open symbols).

in $\text{MgB}_2 + \text{Fe}_2\text{O}_3$ nanocomposite material at 30 K (open symbols) compared to the magnetization loop measured at 42 K. This measurements shows that intrinsic magnetic hysteresis due to magnetic nanoparticles themselves is very small as expected for superparamagnetic material. Also, $M(H)$ curve at 42 K is described well by Langevin function. The hysteresis in a superconducting state is significant even at 30 K. More detailed data including measurements at lower temperatures are shown elsewhere [10], [11]. The solid line in Fig. 3 was obtained by a direct subtraction, $M(H, 30 \text{ K}) - M(H, 42 \text{ K})$. Indeed, it looks just as regular hysteresis curve of a superconductor.

To compare different samples, the measured curves were normalized by the initial slope, $|dM/dH|_{H \rightarrow 0} \approx V/4\pi(1 - N)$, measured at 5 K. Here V is sample volume and perfect diamagnetism is assumed. Fig. 4 compares magnetization loops measured at 30 K in the initial material (solid curve), $\text{MgB}_2 + \text{Mo}_2\text{O}_5$ nanocomposite (solid symbols) and $\text{MgB}_2 + \text{Fe}_2\text{O}_3$ nanocomposite (open symbols). Evidently, both nanocomposite materials show significant enhancement of the magnetic hysteresis. The hysteresis is almost 300% larger in superconductor containing magnetic Fe_2O_3 pinning centers, which implies considerable contribution of magnetic pinning. It is important to note that sonication did not affect the superconducting transition temperature, hence chemical properties of the initial material. Details of this work, including dependence of critical current on slurry loading and amount of obtained nanoparticles is given elsewhere [11].

III. THEORY AND DISCUSSION

A. Finite-Size Ferromagnetic Inclusion in a Superconductor

Surprisingly, there is no theory describing the interaction of ferromagnetic inclusion of finite size in the superconductor's interior with Abrikosov vortices. Early models treated ferromagnetic nanoparticles as point-like zero-dimensional objects which simply modified the mean-field magnetic induction [4]–[6]. For the inclusion of finite size, the situation is considerably more difficult due to nontrivial boundary conditions

and difficulties of describing the microscopic mechanism of interaction of a ferromagnetic nanoparticle with the vortex core. In this paper we ignore complications of the core interactions and look for joint solutions of the London equation in the superconductor bulk and Maxwell equations inside the magnetic particle. Consider a spherical magnetic particle of radius R and magnetization \vec{M} , embedded into an infinite type-II superconductor containing a single straight vortex line at the distance ρ from the center of the particle. The London equation for the vector-potential \vec{A} ($\nabla \times \vec{A} = \vec{B}$, $\nabla \cdot \vec{A} = 0$) in a superconductor, $\vec{A} - \lambda^2 \Delta \vec{A} = 0$ and the Maxwell equation inside the magnetic particle, $\Delta \vec{A} = 0$, can be conveniently solved in spherical coordinates in which vector-potential \vec{A} has only one component $(0, A_\varphi(\rho, \theta), 0)$. The vector potential and tangential component of the magnetic field must be continuous on the particle's surface,

$$\left. \begin{aligned} A_\varphi^{sc}|_{r=R} &= A_\varphi^m|_{r=R} \\ H_t^{sc}|_{r=R} &= H_t^m|_{r=R} \end{aligned} \right\} \Rightarrow (\nabla \times \vec{A}^{sc})_\theta|_{r=R} = (\nabla \times \vec{A}^m - 4\pi\vec{M})_\theta|_{r=R}$$

Here m stands for the solution inside magnetic sphere and sc denotes superconductor. In addition, vector potential should vanish inside a superconductor at $\rho \rightarrow \infty$ and be finite inside the magnetic sphere. The appropriate solution is:

$$\begin{cases} A_\varphi = \frac{4\pi MR \sin \theta}{(1+3(\frac{\lambda}{R})+3(\frac{\lambda}{R})^2)} \frac{(1+\frac{\rho}{\lambda})}{(\frac{\rho}{\lambda})^2} \exp\left(-\frac{(\rho-R)}{\lambda}\right), & \rho \geq R \\ A_\varphi = \frac{4\pi M \rho \sin \theta}{(1+3(\frac{\lambda}{R})+3(\frac{\lambda}{R})^2)} \frac{(1+\frac{\rho}{\lambda})}{(\frac{\rho}{\lambda})^2}, & \rho < R \end{cases}$$

The corresponding supercurrent density induced by the particle at the distance ρ , $4\pi c^{-1} j_\varphi = -A_\varphi \lambda^{-2}$ is:

$$j_\varphi = -\frac{cMR}{(1+3(\frac{\lambda}{R})+3(\frac{\lambda}{R})^2)} \frac{(1+\frac{\rho}{\lambda})}{\rho^2} \exp\left(-\frac{\rho-R}{\lambda}\right) \sin \theta$$

B. Magnetic Pinning Force

Knowing the current density distribution, the magnetic pinning force can be calculated from:

$$\vec{f}_{mag} = c^{-1} \int [\vec{j}(\rho_v, \theta_v) \times \vec{\Phi}_0] dl$$

where integration is carried along the entire vortex. In a general case of an arbitrary orientation, the value of magnetic pinning force is scaled by the factor of $\cos(\alpha)$, where α is the angle of misalignment. In addition, the vortex is experiencing additional moment of forces which is trying to align it along the magnetic moment of the sphere [10]. Results of calculated total magnetic pinning force is shown in Fig. 5 for different sizes of ferromagnetic sphere compared to the penetration depth. The Ginsburg-Landau parameter was chosen $\kappa = 100$, close to the experimental values for MgB_2 [3]. As follows from the calculations, the force experienced by an Abrikosov vortex is attractive and, at larger distances exponentially depends on the separation from the magnetic particle. Compared to the short-range core pinning

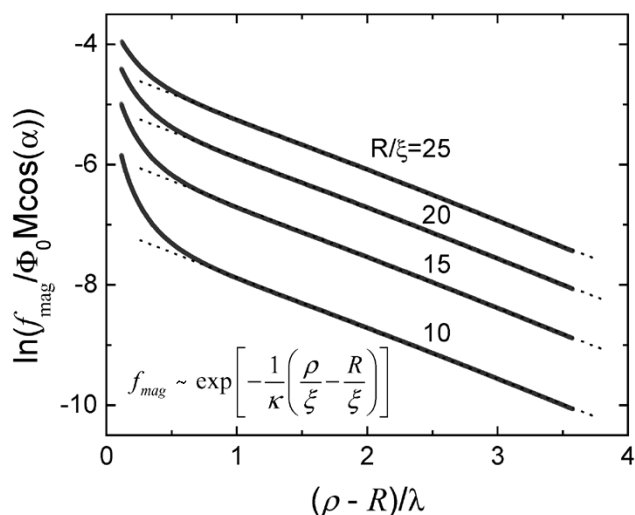


Fig. 5. Magnetic pinning force as a function of the distance between a vortex and a magnetic sphere calculated for spheres of different size.

(effective at distance of the order of the coherence length), magnetic pinning force is long-range (characteristic length scale is the London penetration depth). Since all ferromagnetic nanoparticles also contribute the usual core pinning, such nanosized ferromagnetic nanoparticles are ideal pinning centers.

C. Extension to High- T_c Superconductors

The main technological difficulty of preparing described nano-composite superconducting materials is embedding of ferromagnetic nanoparticles into the bulk of ceramic superconductors. In the case of high- T_c cuprates such as BSCCO and YBCO this issue is crucial, because these materials form variety of phases depending on crystallization conditions. Therefore, direct mixing of nanoparticles into the melt is not feasible (not to mention very large surface tension between the melt and, for example, Fe_2O_3 nanoparticles). Heterogeneous sonochemical synthesis avoids these difficulties by preparing ferromagnetic nanoparticles in situ during the reaction. A more difficult problem is the d-wave nature of high- T_c cuprates. These unconventional superconductors are much more sensitive to magnetism and, therefore, possible contamination of superconducting material with iron during synthesis must be taken into account and the process should be optimized to avoid this effect. One of the ways is to use various gases during synthesis. For example, excess of oxygen binds iron before it has chance to enter the crystal lattice of a superconductor.

Nevertheless, direct effect of sonication on the morphology of high- T_c granular materials is dramatic. Fused together grains and more homogeneous material, indeed, lead to improved superconducting properties. Our recent results show significant enhancement of magnetic and *transport* properties in sonicated BSCCO-2212 [12]. The method has also been adopted for oxygen-sensitive YBCO and yielded promising results.

ACKNOWLEDGMENT

The authors wish to thank K. S. Suslick, V. Geshkenbein, A. A. Polyanskii, A. Gurevich, and B. Ivlev for various discussions.

REFERENCES

- [1] A. M. Campbell and J. E. Evetts, *Critical Currents in Superconductors*. London, U.K.: Taylor & Francis, 1972.
- [2] D. Larbalestier, A. Gurevich, D. M. Feldmann, and A. Polyanskii, "Superconductors: pumping up for wire applications," *Nature*, vol. 414, pp. 368–377, 2001.
- [3] Topical review, "Superconductivity in MgB_2 : electrons, phonons and vortices," *Physica C*, vol. 385, pp. 1–305, 2003.
- [4] T. H. Alden and J. D. Livingston, "Magnetic pinning in a type-II superconductor," *Appl. Phys. Lett.*, vol. 8, pp. 6–7, 1966.
- [5] —, "Ferromagnetic particles in a type-II superconductor," *J. Appl. Phys.*, vol. 37, pp. 3551–3556, 1966.
- [6] C. C. Koch and G. R. Love, "Superconductivity in niobium containing ferromagnetic gadolinium or paramagnetic yttrium dispersions," *J. Appl. Phys.*, vol. 40, pp. 3582–3587, 1969.
- [7] Y. Nozaki, Y. Otani, K. Runge, H. Miyajima, and B. Pannetier, "Magnetostatic effect on magnetic flux penetration in superconducting Nb film covered with a micron-size magnetic particle array," *J. Appl. Phys.*, vol. 79, pp. 6599–6601, 1996.
- [8] M. J. V. Bael, K. Temst, V. V. Moshchalkov, and Y. Bruynseraede, "Magnetic properties of submicron Co islands and their use as artificial pinning centers," *Phys. Rev. B*, vol. 59, pp. 14 674–14 679, 1999.
- [9] J. I. Martin, M. Velez, J. Nogues, and I. K. Schuller, "Flux pinning in a superconductor by an array of submicrometer magnetic dots," *Phys. Rev. Lett.*, vol. 79, pp. 1929–1932, 1997.
- [10] A. Snezhko, T. Prozorov, and R. Prozorov, Magnetic Nanoparticles as Efficient Bulk Pinning Centers in Type-II Superconductors, 2004.
- [11] T. Prozorov, R. Prozorov, A. Snezhko, and K. S. Suslick, "Sonochemical modification of the superconducting properties of MgB_2 ," *Appl. Phys. Lett.*, vol. 83, pp. 2019–2021, 2003.
- [12] T. Prozorov, B. McCarty, Z. Cai, R. Prozorov, and K. S. Suslick, "Effects of high intensity ultrasound on BSCCO-2212 superconductor," *Appl. Phys. Lett.*, vol. 85, pp. 3513–3515, 2004.
- [13] K. S. Suslick and G. J. Price, "Applications of ultrasound to materials chemistry," *J. Annu. Rev. Mater. Sci.*, vol. 29, pp. 295–326, 1999.
- [14] K. S. Suslick and S. J. Doctycz, "Interparticle collisions driven by ultrasound," *Science*, vol. 247, pp. 1067–1069, 1990.
- [15] M. Gagnier, L. Albert, J. Derouet, and L. Beaury, "Ultrasound effects on various oxides and ceramics: macro-and microscopic analyses," *J. Solid State Chem.*, vol. 115, pp. 532–539, 1995.